

# TECHNICAL ARTICLE

# Piping and Pressure Vessel Welding Automation through Adaptive Planning and Control

SAM ROBERTSON  $_{\bigcirc}$ , JOSH PENNEY, J. LOGAN MCNEIL, WILLIAM R. HAMEL, J. DAVID GANDY, GREG FREDERICK, and JON TATMAN<sup>2</sup>

1.—Mechanical, Aerospace, and Biomedical Engineering Department, Tickle College of Engineering, University of Tennessee, Knoxville, Knoxville, TN 37996, USA. 2.—Welding Technology and Repair Center, Electric Power Research Center, Charlotte, NC 28262, USA. 3.—e-mail: whamel@utk.edu

Welding automation is a pathway to reducing costs in the energy sector and dependence on certified welders, who are in short supply. Recent research into system-level automation of multibead/layer Tungsten Inert Gas welding for stainless-steel components is presented. Automation is pursued for weld planning, execution, and defect detection. Planning utilizes active seam/groove sensing and intuitive weld bead positioning. Bead and layer geometries are estimated using weld bead shape prediction that takes into account process parameters. After the first weld layer, subsequent trajectory plans are adapted to compensate for differences between the planned and actual weld surface. Sensor-based, closed-loop control of the process is being pursued to compensate for gravitational effects. Continuous monitoring of the real-time process to predict/detect the occurrence of welding defects is in development. Near-real-time defect detection provides the opportunity for immediate evaluation and correction, reducing costly repairs. Preliminary experimental results are presented.

# INTRODUCTION

Industrial welding is an area of manufacturing that has been highly automated over recent decades. Operations previously performed by human welders are now completely handled by industrial robots in many modern applications. Doing so removes humans from more hazardous working environments and frees up workers for tasks that are not suitable for robots.

In current manufacturing of pipe and reactor pressure vessel (RPV) structures, mechanized approaches utilizing automated torch positioning are employed (orbital typically) but rely primarily on manual and supervisory control by skilled welders. Such reliance on human welders poses a number of issues for the overall process. First, production capacity is limited by the availability of skilled welders, as each welding system requires a dedicated human operator. This need is exacerbated by the current and projected future shortage of qualified and certified welders. 1,2 Additionally, human operators are not well

suited for tedious and continuous process monitoring for quality control judgments, particularly those associated with potential subsurface weld defects. This requires postprocess nondestructive evaluation (NDE) to locate subsurface defects which, if found, require costly and lengthy repair measures before the welded structure can be certified.

Therefore, a higher level of welding process automation—one that maximizes the efficiency of human operators and reduces the necessity for postprocess repair—would significantly benefit piping and pressure vessel manufacturing in all types of power plants. To achieve this level of desired automation (worker optimization and repair reduction), two categories of automated functions must be developed: one that reduces control functions currently performed by humans, and one that seeks near-real-time weld evaluation and defect prediction/identification/correction.

The next section reviews the considerable amount of prior research in the areas of sensing and control that are relevant to the research aims of this work.

Many elements of this prior work provide important foundations and insights, but none have been found that address the overall system-level automation that is sought in this work.

#### PRIOR RESEARCH

Significant research has been conducted on related subjects such as weld modeling, sensing, and control. An overview of weld modeling literature compiled by Babu<sup>3</sup> provides a thoughtful collection of research on modeling. A noticeable issue in current modeling and simulation research is the computational throughput requirements, with the fastest published models running at slightly subminute total execution time scales for simple bead-on-plate simulations.<sup>4</sup> All of the approaches to solving the rigorous governing equations result in computational requirements that cannot be met with the types of embedded computing associated with modern digital control systems.

Similarly, research in the areas of sensing and control for Tungsten Inert Gas (TIG) welding is mainly limited to simple, single pass types of welding. Additionally, research is limited to the control of one aspect of welding (oftentimes penetration)<sup>5,6</sup> instead of treating the holistic process. Literature that aims at more general process control often provides little or ambiguous results. A major focus of sensor- and model-based control research has been vision based, yet it is intuitive that thermal sensing should prove profitable, while some researchers as well as skilled welders assert the usefulness of acoustic sensing. Hence, research into multisensor-based control of the holistic welding process for complex, multipass, multilayer operations is lacking but is needed for technological progression.

An additional consideration for full welding automation is the complexity added by orbital welding. As welding is conducted circumferentially for pipes and pressure vessels, or in any operation that requires welds to be performed out of alignment with gravity, gravitational effects on the fluid flow further complicate modeling, sensing, and control of the welding process as the process dynamics change. These changes are drastic enough that the ASME Boiler and Pressure Vessel Code (ASME BPVC) contains different qualification standards for welds conducted in a variety of nongravity-aligned (NGA) or "out of position" welds. Interest in orbital welding has been consistent for decades due to the production benefits;9,10 however, discussion of control in orbital welding scenarios is generally lacking in literature. Even in research specifically aimed at good welding control results, discussion on gravity compensation in NGA welding positions is omitted.

The remaining sections of this paper are organized as follows: "Welding Automation Concept" section focuses on the functional elements of system-level welding automation, "Experimental

System Description" and "Current Results" sections cover the experimental setup and results obtained thus far, and "Summary and Future Work" section provides a summary and discussion about future work.

#### WELDING AUTOMATION CONCEPT

For comprehensive system-level welding automation, a sensor- and model-based control system that can compensate for dynamic events and disturbances in the welding environment is needed. The general functional architecture of such a system is shown in Fig. 1. Three integrated functional streams are depicted: multibead/layer weld planning, adaptive weld plan execution and control, and parallel weld defect detection. Parallel near-real-time weld defect detection seeks to identify possible defects as they occur, giving operators the opportunity to determine further actions quickly.

# **Weld Planning**

Weld planning is the process of determining the baseline set of beads and layers necessary for a particular job and generating the corresponding weld head/robot trajectories that will place the beads in the proper sequence and locations with respect to the workpiece. To begin, the geometry of the groove or seam to be welded is digitized using a profilometer (a Keyence blue laser profilometer in this case). Since the target of this work is new

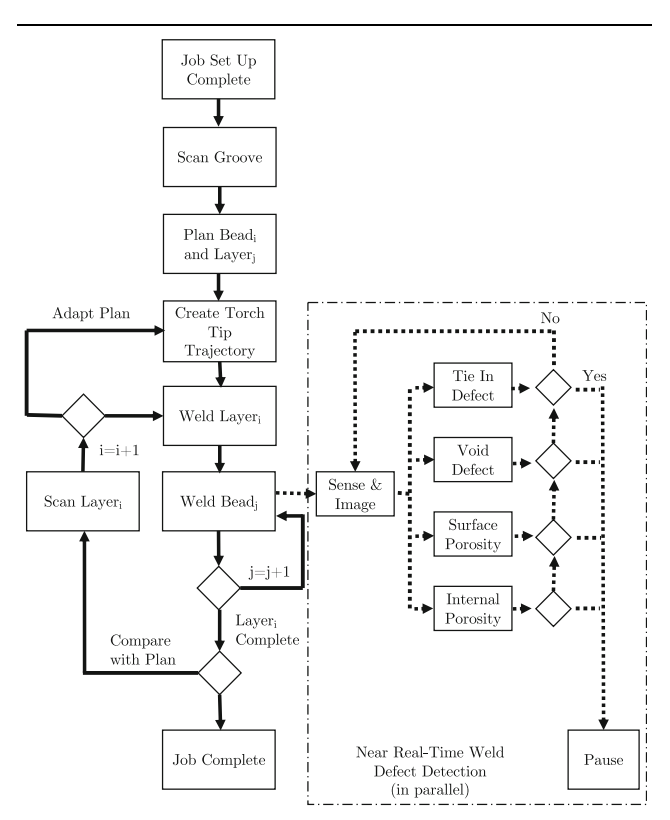


Fig. 1. System functional diagram.

construction fabrication, it can be safely assumed that the prewelded groove geometry is fairly consistent, i.e., that the cross-sectional geometry at any point or segment is representative of the cross-sectional geometry at any other point or segment. This mitigates the need to image the entire joint for planning purposes or to create a complex three-dimensional (3D) plan, utilizing instead a simple three-dimensional plan that simply extends the two-dimensional (2D) section profile along the length of the welds (Fig. 2).

At this point, no welds, other than tack welds, have been performed. Naturally, groove distortions will occur during welding due to thermal expansion, and fit-up deviations may be present. However, these will be handled by the adaptive weld execution control when the results of a specific weld layer are compared with the baseline plan and necessary corrections to the next layer's plan are made.

#### Control-Oriented Weld Bead Modeling

With the groove geometry known, the volume to be filled can be determined as well as the volume and geometry of the cold base metal. This information is combined with the weld process parameters to generate estimations of the weld shapes and cross-sections based on their placement inside the groove (Cartesian position and torch angle in the workpiece space). To produce weld shape estimations within the computational framework of the control system (desktop computer processing rates), a relatively simple weld bead mathematical model is needed. While numerical solutions of the detailed multiphysics governing equations have been used to simulate welding processes in the past, such models can take minutes to hours on high-performance computers to simulate a single bead-on-plate weld. For weld planning in this context, on the order of 30 welds must be simulated in seconds. Therefore, a "control-oriented" parametric bead model that can be realistically executed within the control system embedded computing environment has been developed (and continues to be refined) to link weld parameters and torch tip orientation—with respect to the workpiece—to resulting weld shapes with an accuracy that is sufficient for initial planning and layer-to-layer adaptive corrections.

The automatic job planning algorithm uses the control-oriented weld bead geometry model and the empty groove geometry to specify the position and orientation for each weld bead within its layer as needed to fill the groove to completion. Weld volume, groove volume, tie in, penetration, and overlap requirements are used as inputs to drive an iterative algorithm that determines the number of weld layers required to fill the groove and the optimal

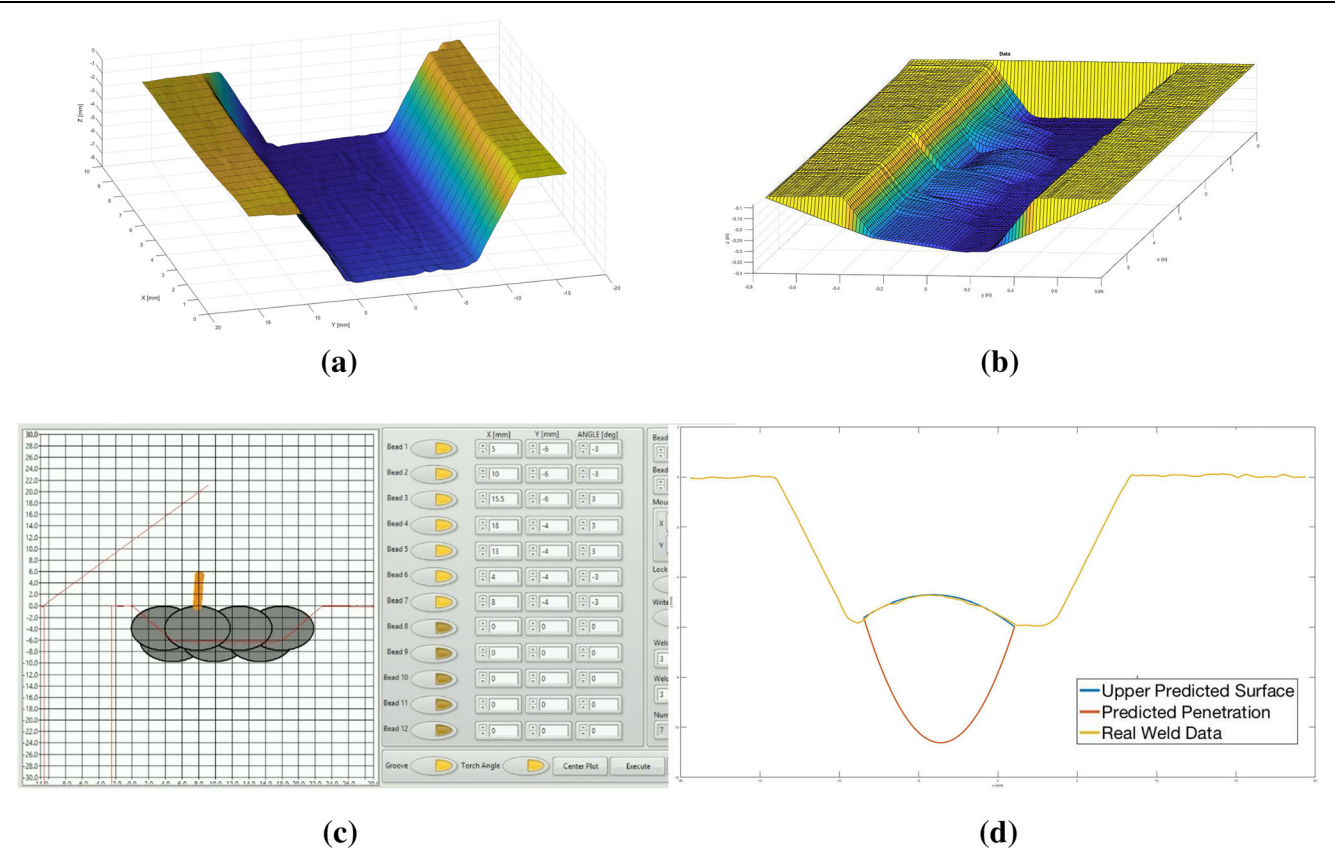


Fig. 2. Weld planning tools and visualization: (a) Keyence profiles stitched into a 3D profile for an empty groove, (b) and a partially welded groove; (c) Graphical weld planning tool; (d) Initial parametric weld model.

bead placement for each weld layer. The results are returned to the system operator for review/modification and approval. Upon approval, the planning system automatically generates the corresponding torch trajectories that are ultimately used as robot servo commands to the Liburdi weld head.

Figure 2 shows the current state of the weld planning and execution interface. For initial work, a simple ellipsoidal weld bead model utilizing bead height and width has been used. However, a parametric model based on the welding parameters and an assumption that abutting parabolas form a reasonable bead profile/penetration estimate has been developed. This model is currently being experimentally evaluated, but utilizes the input power and material flow characteristics of the weld process to generate the upper and lower parabolas that estimate the cross-sectional shape of the weld bead. Work by Tatman et al. <sup>12,13</sup> is the basis for this model; initial results are promising.

### **Adaptive Weld Plan Execution**

Welding operations will begin with the torch tip trajectories from the initial plan. Since the planning process is based on approximate weld bead models, the actual final layer surface will most likely be different from the surface represented in the plan. The plan for the next layer will be adapted to compensate for the previous actual/planned difference based on profilometer characterization of the actual layer geometry. In this way, near-real-time feedback of the actual previous weld layer surface geometry is used to evaluate how well the groove is being filled and the variance between the "planned" and actual welds. The adaptive bead path algorithm (in development) uses inputs from the torch head sensor suite to monitor how the groove is being filled (Fig. 3). The profilometer, mounted a few inches ahead of the torch, digitizes the upcoming groove

geometry, which is used to adjust the torch trajectory plan, ensuring that welds maintain the correct relative position with respect to the groove features and other welds. In addition, knowledge of the torch position combined with the profile scans of prior welds can be used to identify actual (as opposed to estimated) weld geometries. Significant differences will be used to update the bead geometry model and adjust the idealized plan accordingly, resulting in current and future trajectory changes for the welding operations. In extreme scenarios, welds may be added or removed from the plan, but in any scenario in which a significant plan modification is made, the operator is notified by the planning window of the operator interface. When significant differences occur related to the weld bead geometry, the actual geometry will be fed into an algorithm to update the weld bead model.

For both planning and adaptation purposes, as layers are estimated and evaluated, the smoothness and average height of welded layers will be used to make bead path plan adjustments. The average surface height of a given layer should, based on typical weld layer geometries within grooves, be consistent and rather flat. Therefore, for planning purposes, the automated planning routine utilizes the average weld height of the previous layer as the flat surface on which to plan the subsequent layer. During in situ analysis, the actual average height and deviation from the bead profile and geometry between welds in a layer are evaluated; significant deviations and excessive bumpiness are considered indicative of a problem, and welding will be paused for the operator to evaluate the situation.

Figure 2 shows the operator interface for interacting with the weld plans. Bead cross-section estimations are placed inside a cross-section of the empty joint to be welded. Initially, the automated weld planning algorithm displays the planned welding sequence, but prior to execution the operator

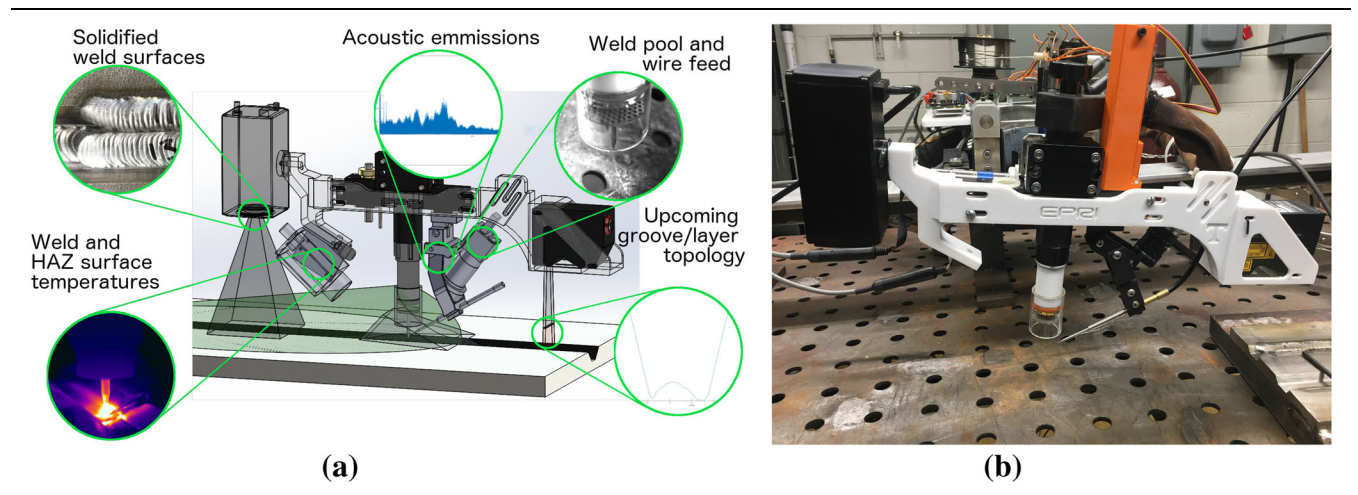


Fig. 3. Experimental testbed (Liburdi F-Head with sensor bracket): (a) modeled sensor placements and fields of functional view; (b) actual system. Sensors (clockwise from bottom left): FLIR thermal camera, CCD camera, microphone, Basler CCD camera, Keyence LJV laser line scanner

will have complete freedom to make modifications with intuitive, point-and-click-style interactions. Once welding begins, the plan is locked, and further manual modifications are halted unless anomalies requiring operator intervention are encountered.

#### **Near-Real-Time Weld Defect Detection**

One of the biggest cost-saving opportunities offered by full welding automation is near-real-time detection of possible weld defects. Early detection will allow defects to be addressed as they occur, making repairs and rework much simpler. The control system will utilize multisensor data fusion to predict the likelihood that one or more common kinds of welding defects have occurred. To begin, four common defect types will be targeted. Table I presents the defects that this system aims to be able to reliably detect. Different defect types can be caused by a variety of factors from improper power settings to a dirty welding environment; however, based on literature concerning the welding process and time spent with highly qualified expert welders, an understanding of which physical features and process signatures characterize welding defects has been developed; <sup>14–16</sup> For example, it is common knowledge among welders that oxides and contaminants can form on the welds' surface and promote formation of internal voids, lack of fusion, and porosity between the layers. Therefore, careful image analysis of the weld layer surface prior to additional welding should be able to identify potential trouble areas, as they will have a different color and reflectivity than the welded metal (Fig. 6; note the strip of surface contaminant on the left-hand side of the leftmost weld).

For algorithm development, welding tests will be conducted, and the process monitored and recorded by a sensor suite consisting of two CCD cameras, a thermal camera, a microphone, and a laser line scanner (Fig. 3; Table I). Additionally, current and

gas flow

voltage data from the arc will be recorded. The thermal camera will be used to trigger interpass wait temperature commands as well as to evaluate the thermal properties of the molten weld pool. This is expected to be useful in the detection of void and internal porosity formation, as cold spots should appear in the liquid and solidifying metal. The microphone will be used to correlate acoustic emissions with the amount of metal (resistance) in the arc circuit. This is useful for both penetration control and determining void formation when pockets change the amount of metal in the circuit. The CCD cameras will be used for judging and controlling torch placement and weld overlap.

All sensed data will be recorded and analyzed to create the control system's understanding of the nominal (good) welding process. Simultaneously, welding tests during which defect-causing conditions will be intentionally introduced will be conducted. The data resulting from these tests will be used to prove and refine the defect prediction algorithms that will be based on a physical understanding of how certain defects form. Multisensor data fusion algorithms will play a large role in developing quick prediction algorithms. Image and audio processing routines will be combined with sensor fusion methods to predict defect formation near the time of occurrence and define the necessary adjustments in the process controls to return to an optimal condition; For example, situations causing internal voids will result in the weld metal not filling in appropriately; a higher surface level (localized) would be expected on top of the void, since that metal has not fused down into the base metal as desired. Additionally, work has been done to correlate arc current and acoustic emission data with the depth of metal under the electrode. Therefore, image processing to evaluate weld height changes can be paired with acoustic and current data processing to predict the likelihood of a void having formed based on the in situ data collection. A

and surface analysis

Defect	Defect types (see Fig. 3 fo	or sensor names a	Correction	Sensor/ Fusion (Potential)	<b>Detection Methods</b>
Surface porosity	Surface contaminants (soot, dirt, etc.), gas flow	Surface bub- ble/cavity; gas	Adjust gas flow; back up and remelt	Visible camera, (micro-	Surface texture and image analysis
Void formation  Poor tie	Surface contaminants, poor placement, material inconsistencies Poor placement	sputter Raised surface; cold spots; acoustic changes Saw-toothed	Remelt; manual grinding and auto- matic reweld Shift torch/wire feed	phone) (FLIR, visible camera, microphone) Visible cam-	Acoustic/electric change correlations and surface analysis Edge detection and
in		edges; gaps	orientation; remelt; filler weld	era, Keyence	differential/frequency analysis
Internal porosity	Surface contaminants, material inconsistencies,	Gas sputter; cold spots; acoustic	Remelt; manual grinding and auto-	(FLIR, micro- phone)	Acoustic/electric change correlations

changes

matic reweld

main question that this research will aim to answer is the resolution of the sensing system with respect to defect formation and detection. While the mechanisms of formation are known, it is as of yet unknown how small of a defect can be detected and at what speed. These concerns are primarily what will be examined and addressed.

Initially, the focus will be on poor tie-in and surface-level porosity, since those will be the easiest to predict or detect due to their surface-level visibility. Poor weld placement is a major factor for tie-in issues and can be partially corrected at the planning stage. Weld beads in the planning stage will be placed to ensure good wetting on the side walls and overlap between beads, so that good fusion is likely. However, even with good planning, real-world deviations can cause planning to go awry. For the in situ tie-in control, the front-facing camera and the rear camera will be utilized. The front-facing camera is aimed at the front of the weld pool where the wire feed enters. This camera angle provides the ability to view the edges of the liquid weld pool. Crowning on the cold edge of the weld bead is indicative of lack of fusion. Additionally, a saw-toothed edge and/or pockets on the weld boundary are indicative of poor fusion and can be identified through image processing of either the rear CCD camera or potentially the rear-facing thermal camera. The image processing to be used will be simple filtering and edge detection to determine whether the weld boundary has deviated from a smooth, straight line along the interface of the current weld and surrounding metal. Under any scenario where poor fusion is detected, the control measure will be for the torch to steer closer to the fusion boundary, which will promote tie-in at a distance based on the width of the defect area (Fig. 6).

# **Out-of-Position Aspects of Orbital Welding**

When performing circumferential welds, as is the case for actual industrial fabrication, gravity effects on the liquid weld pool will pose a challenge for robotic control. To ensure that the welds stay consistent as the welding head moves out of position with respect to the gravitational vector, a weld pool control algorithm is being developed. A somewhat similar control algorithm is being developed using a robotic gas metal arc welding (GMAW) system in another research project within this laboratory. Even though the welding process is different than the TIG system implemented in the groove welding setting, the dynamics of the weld pool are similar. In both cases, a pool of molten metal is in a situation where gravity can influence the flow of the liquid metal and cause the weld pool to change to an undesired shape. This then would result in a misshapen weld bead that would cause defects in the groove. The gravitational effects on the weld pool are typically manifested through a change in

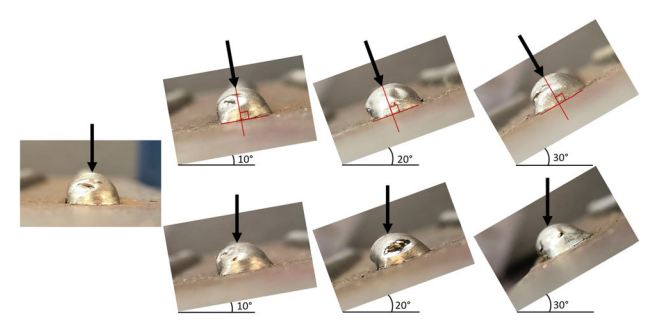


Fig. 4. Comparison of MIG welds at different base plate orientations. The leftmost bead is a control, welded at an angle of 0°. For the welds in the top row, the welding torch was kept perpendicular to the base plate, while for the welds in the bottom row, the welding torch was kept vertical, aligned with the gravitational direction.

geometry with a shift in the direction of gravity (Fig. 4). To combat this change in geometry, there are several different control actions that can be used, e.g., regarding the work angle, the torch angle, and the position of the wire feed with respect to the weld pool. The work angle and torch angle, as well as oscillation and travel speed, allow for manipulation of the orientation of the arc forces against the weld pool, which are corrective measures utilized by skilled human welders as well. By changing how the arc forces are applied to the weld pool, the gravitational forces on the weld pool can be mitigated. This can also be seen in Fig. 4, as the beads welded with the torch oriented perpendicular to the base plate retain a more similar shape to the control bead than the beads welded with the torch aligned with the gravitational direction. The position of the wire feed entry into the weld pool can also assist with more localized control of the weld pool by lowering the temperature of the weld pool at the entry point and thus increasing the surface tension forces in the area around the wire. By increasing the surface tension forces, the resistance of the weld pool to gravitational forces increases, thus helping the weld pool maintain the desired shape.

Further experiments have been run using the GMAW system to test how gravity affects the weld pool in the multilayered case. As can be seen in Fig. 5, as layers continue to be stacked, the gravity effects become more pronounced due to the increase in total heat in the part, as well as the shape of the previous layers. In building the part shown in Fig. 5, the torch was kept perpendicular to the base plate, since this has been shown to produce a bettershaped weld bead than when the torch is aligned with the gravitational direction (Fig. 4). The base plate is angled at 45°, which is more than for the previous welds shown, thus the gravitational effects on the weld pool are stronger. Using these results, further control algorithms are being developed to use feedback from cameras observing the weld pool as well as the known position of the robot to identify when the weld pool is drooping and reorient the torch in a feedback loop that seeks to maintain the desired, ideal weld pool geometry. The resultant



Fig. 5. Example of how gravity affects MIG weld beads in the context of additive manufacturing.

control algorithm will then be updated to use the cameras specific to the TIG groove welding system such that the added control points of the work angle and the wire feed position can also be used to further control the weld pool to produce the desired bead shape in the out-of-position case.

# EXPERIMENTAL SYSTEM DESCRIPTION

Figure 3 shows the experimental system after modifications. The welding system being used for experimental tests and validation of the control system is a Liburdi Dimetrics F style welding head connected to a water-cooled P300 power system. This orbital welding system is designed for mechanized welding not computerized position control, thus significant modifications to the various motor drives were introduced into the system. These modifications included adding servo actuators and control for six axes on the Liburdi and adding a sensor suite mounting bracket.

The sensor mounting bracket has been through several iterations and currently houses a rearfacing Intertest iShot CCD camera (1280 × 720), a rear-facing FLIR A35 thermal camera ( $320 \times 256$ ), a front-facing Basler ACE camera (659  $\times$  494) with a neutral-density filter, a simple microphone mounted to the wire feed arm, and a Keyence LJV blue laser line scanner mounted in front of the welding torch. Since an ultimate goal of this research is commercialization and industrial deployment, all of the system modifications have been made as product agnostic as possible, and the sensors were chosen based on both applicability and cost. A goal is to reduce the number of sensors needed once the control algorithms are developed, to produce as minimal a sensor system as possible.

Several software development environments were explored for this research, and eventually National Instruments LabView software was chosen. It is a coding environment that is easy to use and is designed for sensor-based data acquisition and control, which is a main objective of this research (Fig. 2). A major component of the software control

system under development is a graphical user interface (GUI) for job planning and execution (Fig. 2c). This interface is used for manual and automatic job planning, plan modification and visualization, and execution monitoring and control.

# **CURRENT RESULTS**

### **Weld Planning and Adaptive Execution**

Initial work has been performed to verify the experimental system's ability to reliably perform welds, as well as to evaluate the quality and characteristics of welds performed with minimal to no operator interaction. Dozens of welds were performed in single weld passes and multilayer sequenced groove fills to evaluate the system's performance and note areas in need of enhanced control, as well as identify strategies for control and defect detection that became evident during these tests.

After parameter tests with various sets of welding parameters (current, voltage, travel speed, etc.) were performed, a specific set of parameters was decided on that produced consistent welds in line with what would be desirable, as confirmed by skilled welding technicians and welding engineers at the Electric Power Research Institute (EPRI) in Charlotte, NC. The set of welding parameters chosen was a pulse weld oscillating between 190 amps and 110 amps at 1.3 Hz, 10 V, 3 inches/min travel speed, and a wire speed oscillating between 22 inches/min and 18 inches/min (55.9 cm/min to 45.7 cm/min) in conjunction with the current pulsing. The groove and filler material are both stainless steel, and the filler wire is 0.045"-diameter ER308L. The welds in Figs. 6 and 2d were performed with these weld settings and are generally representative of the shape, size, and surface of welds produced.

Using these welding parameters, two major sets of tests were performed. The first was a series of 20 welds with the same parameters but incrementally different placements laterally within the groove,

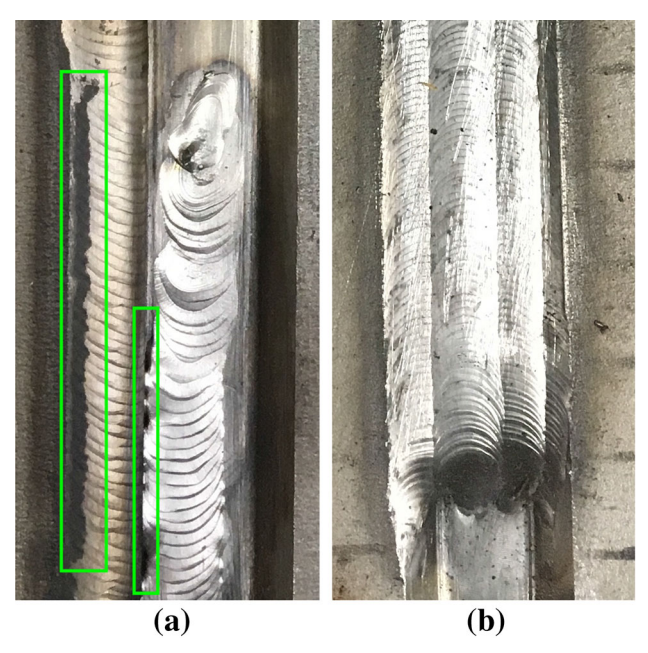


Fig. 6. Resultant test welds. (a) Common weld defects/indicators (saw-toothed edges for poor tie-in; bands of surface contaminants). (b) A successfully filled groove following the open-loop automated filling tests.

from the corner down the sloped walls to the center, and different torch angles towards the wall. Four different angles were used  $(0^{\circ}, 3^{\circ}, 6^{\circ}, \text{ and } 9^{\circ})$  with five welding positions at each angle: two on the sloped wall, two on the flat center, and one in the corner. These welds were performed to evaluate how the weld surface and geometry change with varying torch angle and as a function of location within the groove geometry. Initial analysis indicates that the location in the groove has a more dominant effect on the resulting weld geometry than the torch angle, as welds placed on the walls differ greatly from welds placed in the corner or center of the groove, while welds performed in the same position but with different torch angles are nearly indistinguishable. This is likely due to the varying substrate geometry changing the way heat transfers from the weld pool to the substrate. Pending internal analysis, the torch angle is expected to have a more noticeable role in the geometric characteristics of the weld's penetration due to a directional change of the arc forces.

The second was a series of multilayer, multiweld groove fills using the same welding parameters as the previous tests. During these, a series of welds was planned and executed based on standard practices demonstrated by welding technicians and engineers at EPRI. The welds were then executed automatically by the system, with manual operator intervention occurring only in situations where a system error was encountered. These welds were conducted to evaluate the system's performance without adaptive planning adjustments, and to guide control system development. Errors and faults during these tests also led to modifications

of the hardware and software system and the development of priorities in control system development. Typical welds can be seen in Fig. 6b.

Weld placement remained fairly constant as long as the base plate (substrate) alignment was maintained, but obviously changed in cases where the base plate came out of alignment. To facilitate base plate movements, a robotic control concept called operational space control is employed. In this approach, control decisions must be made with respect to the operational task space of the base plate groove as opposed to the global coordinates of the robot system. Additionally, tests revealed that the wire feeder height is an important feature to control, as variations in previous layer height and stop and start heights on previous weld slopes have a significant effect on what wire feeder height is ideal at any given point. Sensing signatures became evident in relation to this, as the behavior of the wire feeding into the weld pool generates significant and unique acoustic emission frequencies when too high above the weld pool, or grinding into the plate and shaking of the torch head when too low.

Finally, while few surface-level defects were found, after cross-sectioning the welds, voids were discovered in the corner toe of some of the initial layers, indicating the likelihood of poor torch placement. This served to illustrate the need for both process-dependent planning to avoid placement issues and *in situ* void detection to prevent filling over problem areas sans repair.

#### **Weld Defect Detection**

An understanding of welding defects has been developed such that defects can be produced as desired for the purposes of study and detection algorithm development. Initial work has been done to evaluate various image processing routines to identify weld edges and individual welds. A major focus of upcoming experiments and research is the development and validation of defect prediction algorithms. Table I presents the defect types that detection algorithms will be developed for, as well as the sensor cues and sensing modalities that will be employed for each of them.

As mentioned above, surface-visible defects should prove much easier to predict/detect in nearreal time. Porosity is likely to have been caused by poor gas coverage and can be detected visually as well as audially. Since normal gas flow produces a constant-frequency acoustic emission and volumetric rate, turbulent flow problems will be characterized by a sputtering that will change the flow frequency spectrum of the process detectable way. Additionally, pockets in the weld surface will be identifiable via image processing of the solid welds from the rear-facing camera(s). The pockets will both disrupt the smooth edges in an edge-fitting algorithm and differ significantly in color from the surrounding metal, having a darker

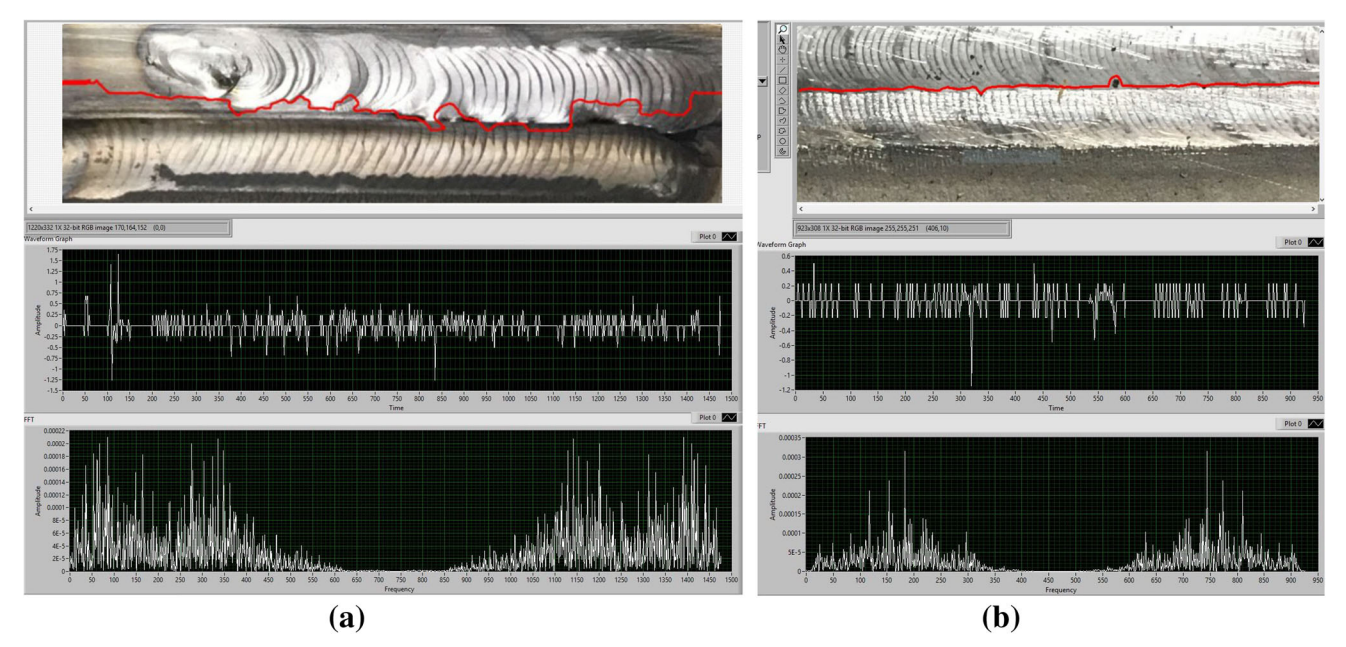


Fig. 7. Image processing and analysis of TIG welds with good and bad tie-in. (a) Jagged and inconsistent edges from poor tie-in (same welds as in Fig. 6a). (b) Straight, even lines with good tie-in (same welds as in 6b but rotated 90°).

pocket of color. In the event of porosity detection, the control system will query the weld power supply to ensure that the gas flow is on and set to the correct rate; if it is not, then operations will be immediately stopped, and the operator will be notified to check the gas supply and connections.

For tie-in control, the main issue is torch tip placement and orientation. The two variables of note are the electrode tip position relative to the groove wall (lateral position) and the angle of the torch towards the base metal. Automatic voltage control of the power supply maintains the torch tip's position relative to the base metal (vertical position) to ensure consistent voltage settings and will therefore not be a control point for the adaptive control system. Based on image processing and the torch position, the edges and perimeter of the weld pool and beads will be identified. Smooth, linear edges are indicative of good tie-in; therefore, similar to porosity, dark spots, holes, and nonlinear edge behavior will be taken as indicative of poor tie-in. However, this should be fixable in situ without stopping operations unless a major inconsistency has developed. The control system, upon detecting poor tie-in, will drive the lateral torch position towards the trouble area to close the gaps and smooth out the edges. This motion will continue until smooth, consistent boundaries between the current and surrounding welds stabilize.

If corrective measures for tie-in on one side of the groove produce a potential tie-in issue on the opposite side of the groove, then the current weld will be driven to a position that provides adequate spacing to ensure appropriate tie-in and fusion will occur during the subsequent weld pass. The trajectory for the fill of the current weld will be updated to

its new position, and the planned welding sequence will be modified for future reference. This will cause the planned operation to change based on the automatic planning routine and will also initiate changes to the weld model. The operator will be notified of the changes and given an option to pause operations.

Initial results for image analysis on welds with good and bad tie-in can be seen in Fig. 7. Seen in both Fig. 7a and 7b are the original image with edge detection overlaid in red. Below the original image is a graph showing the contour variance fit by the edge detection, and below that is the frequency spectrum of the contour variance. As expected, edges with bad tie-in have increased low-frequency content, and generally more frequency content than edges with good tie in, which should have relatively consistent, high-frequency content. This kind of analysis leads into automatic tie-in detection via image processing and edge analysis.

#### SUMMARY AND FUTURE WORK

The initial phase of this research was the conversion of the Liburdi welding head from open-loop velocity control to servo position control and the integration of a multisensor suite suitable for robotics operations. This phase also included the development of an appropriate operator interface and comprehensive data acquisition capability and is essentially complete. A "point and click"-style multibead/multilayer weld planning interface based on a rudimentary weld bead model is now operational.

After the initial phase, work shifted to a focus on the development and testing of adaptive weld planning, weld defect detection, and non-gravityaligned weld pool management algorithms. Preliminary weld tie-in problem detection based on weld surface image processing is showing real promise. Separate research into large-scale additive metals manufacturing based on MIG has provided useful insights into weld pool molten metal behavior associated with non-gravity-aligned welding, which also occurs in orbital TIG welding.

The preliminary results obtained thus far are encouraging and fortify the belief that achieving robust systems-level welding automation using available sensing, control, and robotics technologies is possible in the near future.

### **ACKNOWLEDGEMENTS**

This research is being performed through the NSF Industry/University Cooperative Research Center called the Materials and Manufacturing Joining and Innovation Center (Ma<sup>2</sup>JIC), which is led by the Ohio State University. The specific industry Ma<sup>2</sup>JIC members supporting this work are the Electric Power Research Institute (EPRI), Oak Ridge National Laboratory, and ITW/Miller Electric.

#### REFERENCES

- A. Zalkind, Welding Shortage Fact Sheet. The American Welding Society, Report, (2007).
- J. Wilkey, Blog [Online] (2015). https://awo.aws.org/2015/11/ the-future-remains-bright-for-skilled-welders/. Accessed 11 Nov 2019.
- S. Babu, Introduction to Integrated Weld Modeling, vol 22 (ASM Handbook, Ohio, 2010).
- S. Mishra and T. DebRoy, Tailoring gas tungsten arc weld geometry using a genetic algorithm and a neural network trained with convective heat flow calculations. *Mater. Sci.* Eng. A 454455, 477 (2007).

- N. Lv, J. Zhong, H. Chen, T. Lin, and S. Chen, Real-time control of welding penetration during robotic GTAW dynamical process by audio sensing of arc length. *Int. J. Adv. Manuf. Technol.* 74(1–4), 235 (2014).
- S.B. Chen and N. Lv, Research evolution on intelligentized technologies for arc welding process. J. Manuf. Process. 16(1), 109 (2014).
- J.P. Steele, C. Mnich, C. Debrunner, T. Vincent, and S. Liu, Development of closed-loop control of robotic welding processes. *Ind. Robot Int. J.* 32(4), 350 (2005).
- ASME, ASME boiler and pressure vessel code, Standard (2017).
- R.D. Conroy, Orbital narrow-gap GTAW process is getting noticed. Weld. J. 72(12), 15 (1993).
- B.K. Henon, Orbital GTAW boosts production of leak-free tubing. Weld. J. 85(6), 56 (2006).
- D. Baek, H.S. Moon, and S.H. Park, Development of an automatic orbital welding system with robust weaving width control and a seam-tracking function for narrow grooves. *Int. J. Adv. Manuf. Technol.* 93(1-4), 767 (2017).
- J.K. Tatman, L.S. McCracken, and T.G. Hicks, Development of New Weld Heat Input and Dilution Equations for Gas Tungsten Arc Welding—Part 1, Conference Paper (2013).
- J. K. Tatman, Development of improved equations for weld heat input and dilution control—part 2, conference paper (2018).
- M. Stadler, P. Freton, and J.-J. Gonzalez, Influence of welding parameters on the weld pool dimensions and shape in a TIG configuration. *Appl. Sci.* 7(4), 373 (2017).
- R Komanduri and Z. Hou, Thermal analysis of the arc welding process: Part I general solutions, *Metall. Mater.* Trans. B 31(6), 1353–1370 (2000).
- Y. Li, Y.F. Li, Q.L. Wang, D. Xu, and M. Tan, Measurement and defect detection of the weld bead based on online vision inspection. *IEEE Trans. Instrum. Meas.* 59(7), 1841–1849 (2010).

**Publisher's Note** Springer Nature remains neutral with regard to jurisdictional claims in published maps and institutional affiliations.